Catalytic wet oxidation of H_2S to sulfur on V/MgO catalyst

Eun-Ku Lee[1], Kwang-Deog Jung[2,]*, Oh-Shim Joo[2] and Yong-Gun Shul[1]

[1]*Department of Chemical Engineering, Yonsei University, Seoul 120-749, Korea*
[2]*Eco-Nano Center, Korea Institute of Science and Technology, P.O. Box 131, Cheongryang, Seoul, Korea*

Received 3 June 2004; accepted 11 September 2004

The V/MgO catalysts with different V_2O_5 loadings were prepared by impregnating MgO with aqueous vanadyl sulfate solution. All of the catalysts were characterized by X-ray diffraction (XRD), temperature-programmed reduction (TPR), Raman spectroscopy, and X-ray photoelectron spectroscopy (XPS). It was observed that the H_2S removal capacity with respect to vanadia content increased up to 6 wt%, and then decreased with further increase in vanadia loading. The prepared catalysts had BET surface areas of $11.3 \sim 95.9\ m^2/g$ and surface coverages of V_2O_5 of $0.1 \sim 2.97$. The surface coverage calculation of V_2O_5 suggested that a vanadia addition up to a monomolecular layer on MgO support increased the H_2S removal capacity of V/MgO, but the further increase of VO_x surface coverage rather decreased that. Raman spectroscopy showed that the small domains of $Mg_3(VO_4)_2$ could be present on V/MgO with less than 6 wt% vanadia loading. The crystallites of bulk $Mg_3(VO_4)_2$ and $Mg_2(V_2O_7)$ became evident on V/MgO catalysts with vanadia loading above 15 wt%, which were confirmed by a XRD. The TPR experiments showed that V/MgO catalysts with the loading below 6 wt% V_2O_5 were more reducible than those above 15 wt% V_2O_5. It indicated that tetrahedrally coordinated V^{5+} in well-dispersed $Mg_3(VO_4)_2$ domains could be the active species in the H_2S wet oxidation. The XPS studies indicated that the H_2S oxidation with V/MgO could proceed from the redox mechanism ($V^{5+} \leftrightarrow V^{4+}$) and that V^{3+} formation, deep reduction, was responsible for the deactivation of V/MgO.

KEY WORDS: V/MgO catalyst; wet oxidation; H_2S; surface coverage; redox mechanism.

1. Introduction

Hydrogen sulfide originating from various sources (coal-based power plants, natural-gas processing, refineries, smelter operation) can be regarded as a major air pollutant entering the atmosphere and causing acid rain. Hydrogen sulfide is removed from industrial waste gases via the Claus process [1,2].

$$2H_2S + SO_2 \leftrightarrow (3/n)S_n + 2H_2O$$

Thermodynamic limitations of the Claus equilibrium reaction led to the development of new processes to deal with the Claus tail gas. The importance of tail gas clean-up processes has been emphasized to meet stricter environmental regulations [3]. Several heterogeneous catalytic systems have been commercialized for the tail gas clean-up process. The Superclaus and BSR were developed for the direct oxidation of H_2S to sulfur above dew point [4,5]. Catalysts containing vanadium oxide have been reported to be active for the oxidation of H_2S to sulfur [6–9]. It has been suggested that *the generation of vanadyl sulfate ($VOSO_4$) is one reaction of the deactivation*. And it was also reported that the reduction of vanadium oxide could be another cause of the deactivation [10]. Various binary oxides such as V–Mg, V–Bi, V–Mo, V–Sb, Fe–Sn and Bi–Mo were tested in excess oxygen without water [11,12]. Solid solutions of vanadium, $A_4 \pm yV_2 \pm xO_9$ (A = Mg, Ca or Zn, $0 \leq x \leq 0.2, 0 \leq y \leq 0.5$) [13,14] were also reported as active catalysts, even in the presence of 30 vol.% of water. The heterogeneous catalytic systems for the processes showed the high activity, but the high reaction temperature resulted in the low stability of the catalysts by the sulfidation of metal and metal oxide components as well as in the low selectivity by the formation of SO_2.

Another approach is using the wet oxidation processes. These have some advantages over other processes in terms of simplicity and performace. The developed processes are using either a V^{5+}/V^{4+} couple (Stretford and Unisulf) or a Fe^{3+}/Fe^{2+} couple (Lo–Cat, Lo–Cat II, Sulferox, and Bio–SR) with chemicals for stabilizing the vanadium, or iron [13–20].

Recently, we developed a new type of room temperature catalyst, Fe/MgO [21,22], which gave a high removal capacity of H_2S. The high H_2S removal capacities of Fe/MgO could be explained by the finely dispersed iron oxide on MgO support. In the present study, we investigated the vanadia loading effect on MgO for the H_2S wet oxidation at the room temperature. The prepared V/MgO catalysts were characterized to correlate the physical and structural properties of V/MgO catalysts with the activity of H_2S wet oxidation.

2. Experimental

The V/MgO catalysts were prepared by an impregnation of MgO (Aldrich 34279) with aqueous vanadyl

---

*To whom correspondence should be addressed.
E-mail: jkdcat@kist.re.kr

1011-372X/04/1200–0259/0 © 2004 Plenum Publishing Corporation

sulfate solutions, followed by drying at 100 °C and subsequent calcinations in air for 5 h at 460 °C.

Activity measurements were carried out using a stirred batch tank reactor. The catalyst samples (3.0 g, if not specified) were dispersed in the reactor charged with the distilled water (1.5 L, if not specified) and the reactant gases were supplied through a perforated rubber plate at the bottom of the reactor. H_2S concentrations from the reactor were measured with on-line G.C with FPD detector which can detect up to 0.1 ppm H_2S. Porapak Q column (118″ O.D × 2 m) was used for separating the product gases.

The specific surface areas of the catalysts were obtained in an ASAP 2000 apparatus, using the BET method from the nitrogen adsorption isotherms at 77 K, taken a value of 0.164 nm^2 for the cross-section of nitrogen.

XRD patterns were collected with Rint 2000 (Rigaku, Co.) using Cu Kα radiation ($\lambda = 0.1542$ nm).

Raman spectra were obstained using a HoloLab Series 5000 Raman spectrometer (Kaiser Optical) equipped with an Nd TAG laser frequency doubled to 532 nm. The catalyst was pressed into a wafer around 0.1-cm thick and 0.9 cm diameter and then placed within a quartz cell. The lazer was operated at a power level of 75 mW. The Raman spectrum was recorded after treating the sample at 773 K in a He flow for 1 h and cooling it to room temperature.

Temperature-programmed reduction experiments were carried out in a micro-reactor system with a TCD detector. Samples of 50 mg were first treated in argon at room temperature for 1 h. After that, the samples were reduced in a stream of 5% H_2/Ar (30 mL/min) at a ramping rate of 20 °C/min from 100 to 1200 °C.

XPS spectra were obtained using a Kratos XSAM 800pci X-ray photoelectron spectrometer with Al Kα monochromatic X-ray (l487 eV) radiation. The charging effect of XPS spectra was carefully corrected with adventitious carbon at 284.6 eV as a reference.

3. Results and discussion

Figure 1 shows the H_2S removal behavior of the V/MgO catalysts with different vanadia loadings. No sulfur oxides were detected in the exit gas streams, indicating that the oxidation of H_2S to SO_2 can be prevented in the wet catalytic oxidation [23]. The H_2S removal efficiency of the V/MgO catalysts maintains above 99% up to 13 h. The activity in H_2S wet oxidation increases up to 6 wt% vanadia loading, and then decreases with further increase in vanadia loading.

In order to investigate changes in surface areas caused by different vanadia loadings, the BET surface areas of V/MgO catalysts were measured. Table 1 shows the physical properties of V/MgO samples. As the loading of vanadia increases from 1 to 30 wt%, the BET surface area decreases from 95.9 to 11.3 m^2 /g and the surface coverage of VO$_x$ increases from 0.5 to 14.4 V atms/nm^2, assuming all of the vanadium is exposed on the surface. The observed decrease in surface area with increase in vanadia loading is similar to that reported previously for the V/MgO catalysts prepared by a impregnation method [24–27]. It is probably caused by dispersion of vanadia which leads to plugging of micropores of MgO support [28,29].

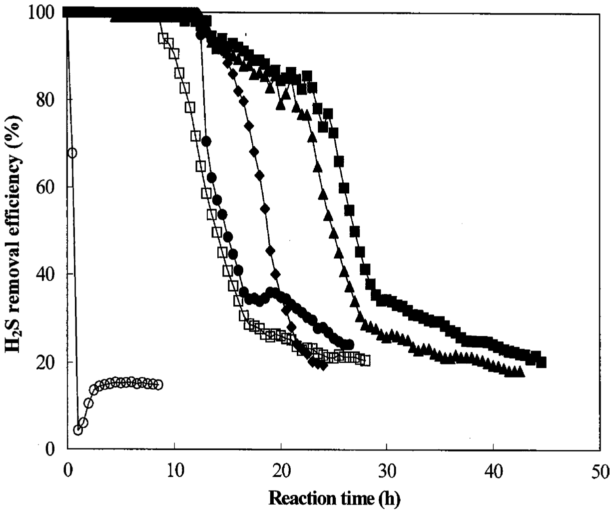

Figure 1. H_2S removal capacities with 1 wt% V/MgO (◆), 4 wt% V/MgO (*triangle*), 6 wt% V/MgO (■), 15 wt% V/MgO (●), 30 wt% V/MgO (□), and MgO (○) in H_2S wet catalytic oxidation. H_2S flow rate: 5 mL/min, O_2 flow rate: 100 mL/min.

Table 1
Physical characterization of V/MgO samples

Sample	V_2O_5 (wt%)	S_{BET} (m^2/g)	Pore volume (cm^3/g)	Average pore diameter (Å)	Average surface coverage[a]	
					V atoms nm^{-2}	As a fraction of V–O monolayer
MgO	–	137.5	0.30	154.3	–	–
1 V/MgO	1	95.9	0.42	147.4	0.5	0.10
4 V/MgO	4	76.7	0.36	153.1	1.9	0.40
6 V/MgO	6	69.9	0.29	150.7	2.9	0.59
15 V/MgO	15	16.1	0.07	173.9	7.2	1.49
30 V/MgO	30	11.3	0.04	181.2	14.4	2.97

[a] $\Phi_{vo2.5} = 0.103$ nm^2.

The expected average surface coverage of vanadia on MgO after dispersion was calculated on the basis of the BET surface areas as shown in table 1, where surface area per $VO_{2.5}$ unit in the (010) plane (0.103 nm^{-2}) was assumed to calculate the fraction of V–O monolayer [30]. It is noted that, in the samples above 15 wt% V_2O_5, values of average surface coverage are higher than the number of equivalents of V–O monolayer. The decrease in H_2S removal capacity of 15 wt% V/MgO catalyst can be ascribed to the formation of multilayer of vanadia.

Figure 2 shows XRD patterns for the V/MgO catalysts after calcinations at 460 °C. All of the samples show the peaks attributable to MgO (JCPDS 4–829). In the case of the sample containing 15 wt% V_2O_5, two peaks appear between 25 and 30°, which are attributed to partially crystallized $Mg_2(V_2O_7)$ (JCPDS 29–877). And the peak at 35° with low intensity is related to the presence of poorly crystalline $Mg_3(VO_4)_2$ phase (JCPDS 19–779) [31]. The intensity of these peaks increase with an increase in vanadia loading. Two Mg vanadate phases such as $Mg_3(VO_4)_2$ and $Mg_2(V_2O_7)$ were found to be present in MgO at high V_2O_5 loadings [32,33].

Figure 3 shows Raman spectra of the V/MgO catalysts calcined at 460 °C. The peak at 860 cm^{-1} can be assigned to a tetrahedrally coordinated VO_4^{3-} species with V/MgO catalysts below 6 wt% V_2O_5 [33,34]. At a loading of 15 wt%, together with the peak at 860 cm^{-1}, new peaks are observed at 380 and 1020 cm^{-1}. The peaks at 380 and 860 cm^{-1} are attributed to $Mg_3(VO_4)_2$, whereas the appearance of the band at 1020 cm^{-1} is attributed to $Mg_2(V_2O_7)$ [28,34]. The intensity of these peaks increase with increasing vanadia loading up to 30 wt%. At high loadings above 15 wt%, $Mg_3(VO_4)_2$ and $Mg_2(V_2O_7)$ are found to be the dominant structures on the surface. The high removal capacity of H_2S (figure 1), XRD (figure 2) and Raman spectra (figure 3) suggest that well dispersed $Mg_3(VO_4)_2$ phases are active species, while the crystallites of $Mg_3(VO_4)_2$ and $Mg_2(V_2O_7)$ phases are inactive in H_2S wet oxidation.

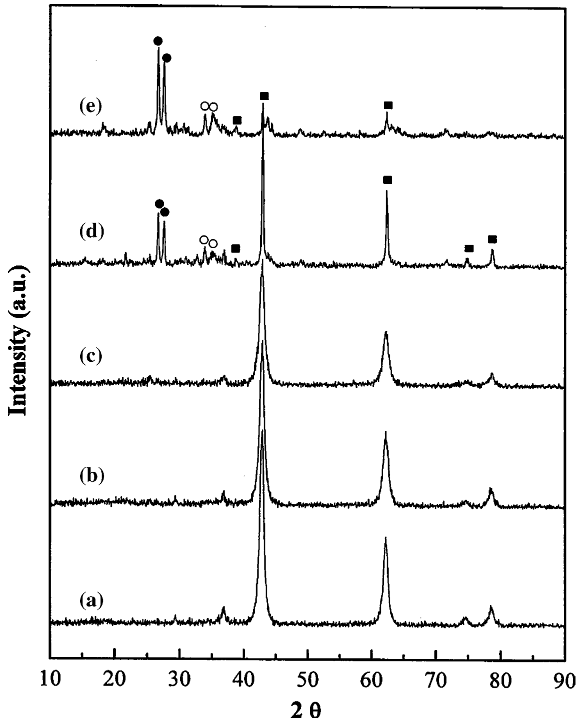

Figure 2. X-ray diffraction patterns of (a) 1 wt% V/MgO, (b) 4 wt% V/MgO, (c) 6 wt% V/MgO, (d) 15 wt% V/MgO, and (e) 30 wt% V/MgO:(●) MgO; (○) $Mg_3(VO_4)_2$; (*let*) $Mg_2(V_2O_7)$.

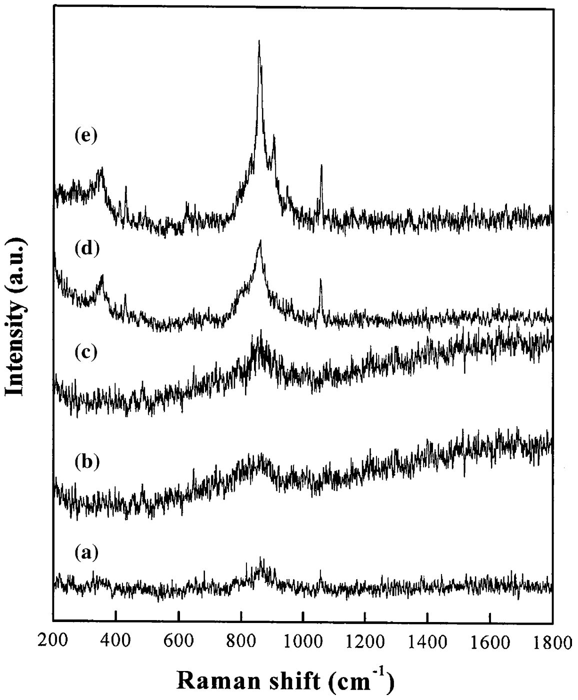

Figure 3. Raman spectra of (a) 1 wt% V/MgO, (b) 4 wt% V/MgO, (c) 6 wt% V/MgO, (d) 15 wt% V/MgO, and (e) 30 wt% V/MgO.

Figure 4 shows TPR profiles for 1 wt% V/MgO sample, the peak is observed at ca. 700 °C. With increasing vanadia loading up to 6 wt%, the peak slightly shifts from 700 to 710 °C [35,36]. The further vanadia loading, 15 wt% V/MgO, shows the peak at 878 °C with a shoulder peak at 816 °C, indicating that new phases can be formed. The TPR profiles in figure 4 are similar to those reported previously for V–Mg–O prepared by aqueous impregnation [36]. TPR peaks at at 690 ~ 710 °C can be assigned to the reduction of tetra-

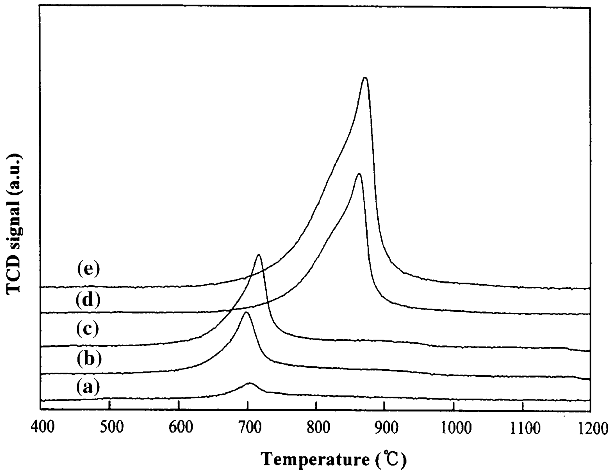

Figure 4. TPR profiles of (a) 1 wt% V/MgO, (b) 4 wt% V/MgO, (c) 6 wt% V/MgO, (d) 15 wt% V/MgO, and (e) 30 wt% V/MgO.

hedrally coordinated V^{5+} in well dispersed small domains of $Mg_3(VO_4)_2$ which are observed in Raman spectra. The TPR peak at 878 °C can be assigned to the reduction of V^{5+} in crystalline $Mg_2V_2O_7$ [33]. The formation of $Mg_2(V_2O_7)$ may result in the shift of the peak temperature for reduction. It is notable that the vanadium cations in crystalline become more difficult to be reduced. It can be explained by the in-accessibility of the reducing agent to the oxygen atoms associated with the Mg vanadate domains below the oxide surface as the size of vanadate [36]. It was reported that the peak temperature for the reduction of bulk $Mg_2(V_2O_7)$ was higher than that for $Mg_3(VO_4)_2$ supported on MgO [33]. In that point of view, the shoulder peak at 816 °C can be assigned to crystalline $Mg_3(VO_4)_2$. The XRD patterns and Raman spectra support that these domains for the loading above 15 wt% V_2O_5 are evident.

As shown figure 4, the $Mg_3(VO_4)_2$ increases together with isolated VO_4^{2-} species up to a vanadia loading of 6 wt%. The steady increase in H_2S removal capacity seen in figure 1 up to a vanadia loading of 6 wt% suggests that isolated VO_4^{2-} units and the dispersed $Mg_3(VO_4)_2$ are active phases for H_2S oxidation. It is observed that a considerable decrease in the H_2S removal capacity occurs with increase in the loading from 6 to 15 wt% V_2O_5. Raman spectra and XRD show that the characteristic peaks of crystalline $Mg_2V_2O_7$ and $Mg_3(VO_4)_2$ appear with an increase in the vanadia loading from 6 to 15 wt%. Therefore, it can be suggested that the reducibility of V^{5+} in vanadia can be related to the H_2S removal capacity of V/MgO catalysts.

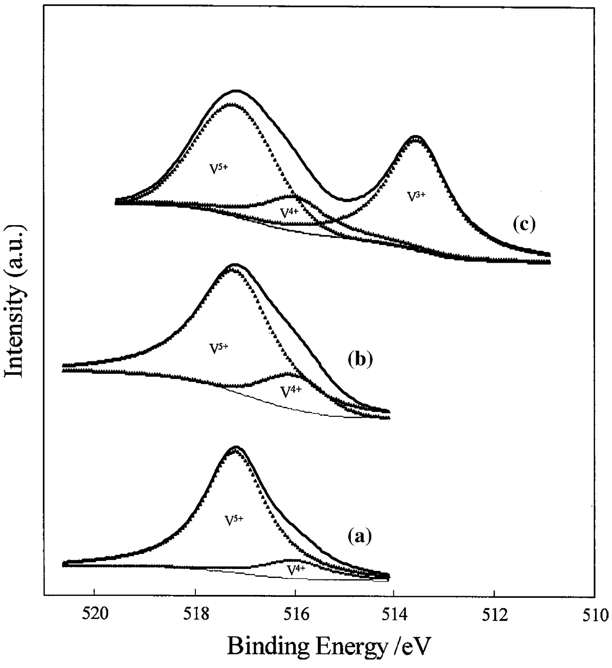

Figure 5. XPS spectra of (a) V/MgO after 4 h reaction, (b) V/MgO after 12 h reaction, and (c) V/MgO after 30 h reaction.

The XPS spectra were obtained for the observation of changes in the catalyst surface after reactions. Figure 5 shows the XPS spectra of the 6 wt% V/MgO catalysts after 4, 12, and 30 h reaction. XPS peaks of V $2p_{3/2}$ for V^{5+}, y^{4+}, and V^{3+} are located at 517.2, 515.9 and 513.5 eV, respectively [32,37,38]. Vanadium component in a fresh V/MgO catalyst is in the state of V^{5+}. Vanadium valence states in V/MgO catalyst changes from V^{5+} to V^{3+} via V^{4+} during the reaction. Such results indicate that H_2S can reduce V^{5+} to V^{3+} at room temperature.

It has been reported that liquid redox process use the reduction/oxidation cycle, as the followings [14,22].

$$H_2S + 2V^{5+} \rightarrow S + 2H^+ + 2V^{4+} \quad (1)$$

$$1/2O_2 + 2V^{4+} + 2H^+ \rightarrow 2V^{5+} + H_2O \quad (2)$$

The V^{5+} is reduced to V^{4+} by H_2S, where the V^{4+} is regenerated back to V^{5+} via a re-oxidation reactions involving oxygen on the heterogeneous catalyst as shown in Fe/MgO [22]. The reduction degree of the V/MgO catalyst during the reaction can be governed by the relative magnitudes of the reduction rate by H_2S with the oxidation rate by oxygen. However, the observation of large amount of V^{3+} valence state in the deactivated catalyst suggests that the deactivation of V/MgO can be due to deep reduction of vanadium oxide by H_2S.

Figure 6 shows the effects of (a) O_2 partial pressure and (b) H_2S partial pressure of the 6 wt% V/MgO for

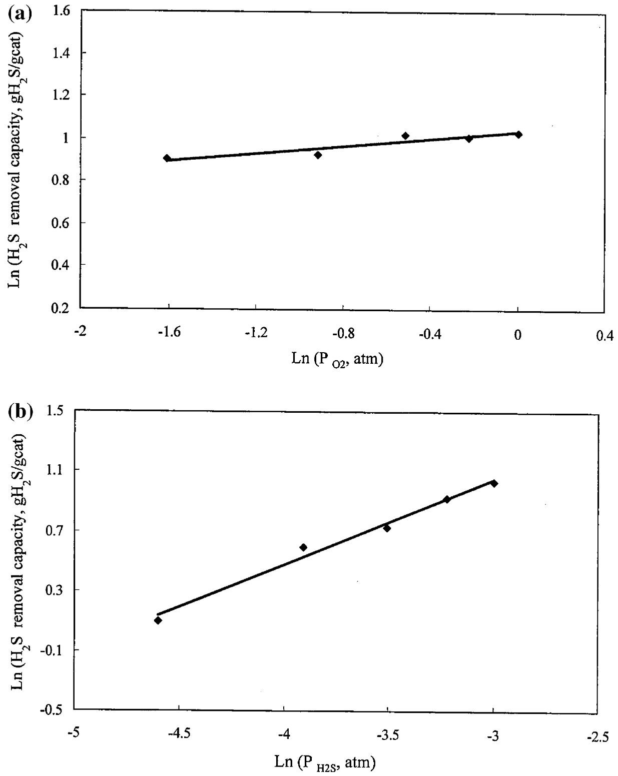

Figure 6. Dependency of (a) O_2 partial pressure and (b) H_2S partial pressure of V/MgO for H_2S oxidation reaction on the H_2S removal capacity.

H_2S wet oxidation. The catalyst sample was dispersed in the stirred tank reactor charged with 1.5 L water. For the investigation of the O_2 partial pressure effect, H_2S (5 mL/min) was introduced with O_2-N_2 mixture (100 mL/min) into the reactor at room temperature. O_2 (100 mL/min) was introduced with H_2S-N_2 mixture (5 mL/min) into the reactor for the investigation of the H_2S partial pressure effect. The removal capacity is defined as the H_2S weight removed per 1 g catalyst.

Logarithmic H_2S removal capacity of the V/MgO catalyst is plotted with respect to logarithmic oxygen partial pressure in figure 6a. The dependency of 0.08 ± 0.005 order of the oxygen partial pressure on the H_2S removal capacity is calculated from the plot. The H_2S removal capacity of the V/MgO catalyst is 2.8 ± 0.05 g H_2S/g_{cat} in a stream if O_2 and 2.5 ± 0.05g H_2S/g_{cat} in the stream of air. The order of the H_2S partial pressure on the breakthrough capacity of the V/MgO catalyst is obtained to be 0.57, indicating that H_2S removal capacity is dependent on the H_2S partial pressure as shown in figure 6b.

The dependency of H_2S partial pressure supports that the reducibility of vanadia on V/MgO can be closely related to the H_2S removal capacity.

4. Conclusions

The V/MgO catalysts with different (1, 4, 6, 15, and 30 wt%) vanadia loadings were prepared by impregnation of aqueous vanadyl sulfate solution on MgO support. The H_2S removal capacity was maximized with 6 wt% V/MgO. The structural analysis suggest that a well dispersed vanadia can be active phase and crystalline $Mg_3(VO_4)_2$ and $Mg_2(V_2O_7)$ should be avoided for H_2S oxidation. XPS study shows that the H_2S oxidation with V/MgO can be explained by the redox mechanism and the deep reduction of V^{5+} to V^{3+} can be responsible for the deactivation of V/MgO. The dependency of H_2S partial pressure supports that the reducibility of tetrahedrally coordinated V^{5+} in isolated VO_4^{2-} species or V^{5+} in a well dispersed small $Mg_3(VO_4)_2$ domain can be closely related to the H_2S removal capacity of V/MgO.

References

[1] J.W. Estep, G.T. McBride and J.R. West, West, Advances in Petroleum Chemistry and Refining, Vol. 6, (Interscience, New York, 1962) 315 pp.

[2] B.G. Goar, Oil Gas 25 (1975) 96.

[3] Anon, Sulfur 20 (1995) 236.

[4] P.F.M.T. Van Nisselrooy and J.A. Lagas, Catal. Today 16 (1993) 263.

[5] V.I. Marshneva and V.V. Mokrinskii, Kinet. Catal. 29 (1988) 989.

[6] R.H. Hass, R.C. Hansford and H. Henning, US patent 4088 (1978) 473, to Union Oil Company.

[7] K.T. Li, M.Y. Hyang and W.D. Cheng, Ind. Eng. Chem. Res. 35 (1996) 621.

[8] K.T. Li, C.S. Yen and N.S. Shyu, Appl. Catal. A 156 (1997) 117.

[9] K.T. Li, M.Y. Hyang and W.D. Cheng, US patent 5653953 (1997), to Tunghai University, Taiwan.

[10] M.S. Shin, C.M. Nam, D.W. Park and J.S. Chung, Appl. Catal. A 211 (2001) 213.

[11] R.A. Bouyanov, A.M. Tsyboulesky, B.P. Zolotovsky, D.P. Klevtsov and V.I. Mourine, US Patent 5369076 (1994), to Institut de Rcherches de Gas Narurels.

[12] R.A. Bouyanov, A.M. Tsyboulesky, B.P. Zolotovsky, D.P. Klevtsov and V.I. Mourine, US Patent 5512258 (1996), to Institut de Rcherches de Gas Narurels.

[13] D.A. Dalrymple, T.W. Trofe and D. Leppin, OGJ 23 (1994) 54.

[14] M.P. Quinlan and D. Leppin, AIChE Spring National Meeting, New Orleans, 2 (1993).

[15] J.E. Johnson, S.J. Tzap, R.E. Kelley and L.P. Laczko, OGJ 22 (1993) 20.

[16] W. Kensell and D. Leppinin Proceedings of the 7th GRI Sulsur Recovery Conference, 1995.

[17] L.C. Hardison, AIChE Spring National Meeting, New Orleans, 2 April 1993.

[18] B.G. Goar and E. Nasato, OGJ 23 (1994) 61.

[19] J.B. Lefers, W.T. Koestsier and W.P.M. van Swssij, Chem. Eng. J. 15 (1978) 111.

[20] D.W. Newman and S. Lynn, Am. Inst. Chem. Eng. J. 30 (1984) 62.

[21] K.D. Jung, O.S. Joo, S.H. Cho and S.H. Han, Appl. Catal., 240 (2001) 213.

[22] K.D. Jung, O.S. Joo and C.S. Kim, Catal. Letters 84 (2002) 53.

[23] K.D. Jung, Characterization of Fe/MgO for wet catalytic oxidation, ACS meeting, Chicago. Augest 2001.

[24] D.S.H. Sam, V. Soenen and J.C. Volta, J. Catal. 123 (1990) 417.

[25] P.M. Michalakos, M.C. Kung and H.H. Kung, J. Catal. 140 (1993) 226.

[26] A. Khodakov, J. Yang S. Su, E. Iglesia and A.T. Bell, J. Catal. 177 (1998) 343.

[27] A. Khodakov, B. Olthof, A.T. Bell and E. Iglesia, J. Catal. 181 (1999) 205.

[28] A. Corma, J.M. Lopez Nieto and N. Paredes, J. Catal. 144 (1993) 425.

[29] A. Corma, J.M. Lopez Nieto, N. Paredes, A. Dejoz and I. Vasquez, Stud. Surf. Sci. Catal. 82 (1994) 113.

[30] F. Roozeboom, M.C. Mitteimeijer-Hazeleger, J.A. Moullin, J. Medema, V.H.J. de Beer and P.J. Gellings, J. Phys. Chem. 84 (1980) 2783.

[31] T. Blasco, A. Dejoz, J.M. Lopez Nieto and M.I. Vazquez, J. Catal. 157 (1995) 271.

[32] X. Gao, P. Ruiz, Q. Xin, X. Guo and B. Delmon, J. Catal. 148 (1994) 56.

[33] M.K. Yurdakoc, R. Haffner and D. Honicke, Mater. Chem. Phys. 44 (1996) 273.

[34] G. Deo and I.E. Wachs, J. Phys. Chem. 95 (1991) 5889.

[35] P. Concepcion, J.M. Lopez Nieto and U. Perez-Pariente, J. Mol. Catal. A 97 (1995) 173.

[36] P. Chanho, A.T. Bell and T.D. Tilley, J. Catal. 206 (2002) 49.

[37] N.K. Nag and F.E. Massoth, J. Catal. 124 (1990) 127.

[38] H.K. Matralis, M. Ciardelli, M. Ruwet and P. Grange, J. Catal. 157 (1995) 368.